NANO LETTERS

2009
Vol. 9, No. 9
3096-3099

Signal Amplification by 1/*f* Noise in Silicon-Based Nanomechanical Resonators

Diego N. Guerra, Tyler Dunn, and Pritiraj Mohanty*

Department of Physics, Boston University, 590 Commonwealth Avenue, Boston, Massachusetts 02215

Received February 11, 2009; Revised Manuscript Received June 22, 2009

ABSTRACT

We report signal amplification by 1/f^{α} noise with stochastic resonance in a nonlinear nanomechanical resonator. The addition of 1/f^{α} noise to a subthreshold modulation signal enhances the probability of an electrostatically driven resonator switching between its two vibrational states in the hysteretic region. Considering the prevalence of 1/*f* noise in the materials in integrated circuits, signal enhancement demonstrated here, using a fully on-chip electronic actuation/detection scheme, suggests beneficial use of the otherwise detrimental noise.

Colored noise with a 1/*f* spectrum is ubiquitous in nature. First discovered in vacuum tubes over eight decades ago,[1] this so-called 1/*f* noise is observed in a wide range of mechanical, geological, biological, and astrophysical systems. Examples of 1/*f* noise include distribution of stars in a galaxy,[2] movement of tectonic plates,[3] statistics in a DNA sequence,[4] rhythm of heartbeats in most living systems,[5] and the random opening and closing of ion channels in the cell membrane in the brain,[6] the channel noise in neurons. In condensed matter systems and solid materials, 1/*f* noise plays a rather significant role. In a wide range of systems, from standard commercial bulk complementary metal oxide semiconductor (CMOS) circuits[7] to Josephson-junction quantum bits,[8] influence of 1/*f* noise is detrimental to the device performance due to its unavoidable presence in the material itself. This has resulted in a lot of research activities, primarily focused on mitigating its presence and influence. In a fundamentally different approach, we ask the following question: Can 1/*f* noise in a device be used to increase the signal-to-noise ratio, for instance, by stochastic resonance?[9] If it is possible, then the intrinsically generated 1/*f* noise in a semiconductor device can be positively exploited for better device performance.

One technology particularly well suited for such a study is nanoelectromechanical systems (NEMS), whose potential application as a two-state system such as a memory element[10] or a switch[11] will rely on integrated circuitry to facilitate operation. Here, we demonstrate signal amplification by 1/*f* noise in switching between the two vibrational states of a silicon-based nanomechanical resonator in the hysteretic regime. The addition of 1/*f* noise to a subthreshold signal produces stochastic resonance, where the likelihood of switching between the two states is maximized for a particular noise power. The engineered nanomechanical two-state systems are somewhat similar to a neurobiological system-rat skin neurons-in the effect that colored noise has on stochastic resonance.[12]

Previously, signal amplification by stochastic resonance in silicon nanomechanical resonators has been observed only in presence of white noise.[13,14] Even though these studies established the fundamental approach of using stochastic resonance for signal enhancement in nano- and micromechanical devices, the demonstration was carried out with magnetic actuation with superconducting magnets at subkelvin temperatures[13] or with laser-based optical readouts.[14] Here, the prototypical silicon device is actuated and detected by standard electrostatic actuation at room temperature.

Our devices are fabricated by e-beam lithography and standard nanomachining, from single crystal silicon using a silicon-on-insulator (SOI) wafer. Figure 1 includes a micrograph of the device, showing actuation and detection electrodes and the central beam, which is 20 μm long, 300 nm wide, and 500 nm thick. The gap between the beam and the electrodes is 250 nm. Actuation and detection of the beam are achieved by the standard electrostatic technique[11] (and references therein) (Figure 1b). A voltage at megahertz frequency applied to the actuation electrode produces the in-plane motion of the beam. With the beam biased at constant voltage (V_B = 17 V for all results), this motion induces a current, $i = V_B\dot{x}(dC/dx)$ at the detection electrode, where C is the capacitance between the beam and the electrode, and x is the effective displacement of the beam.

* To whom correspondence should be addressed. E-mail: mohanty@physics.bu.edu.

10.1021/nl9004546 CCC: $40.75
Published on Web 08/17/2009

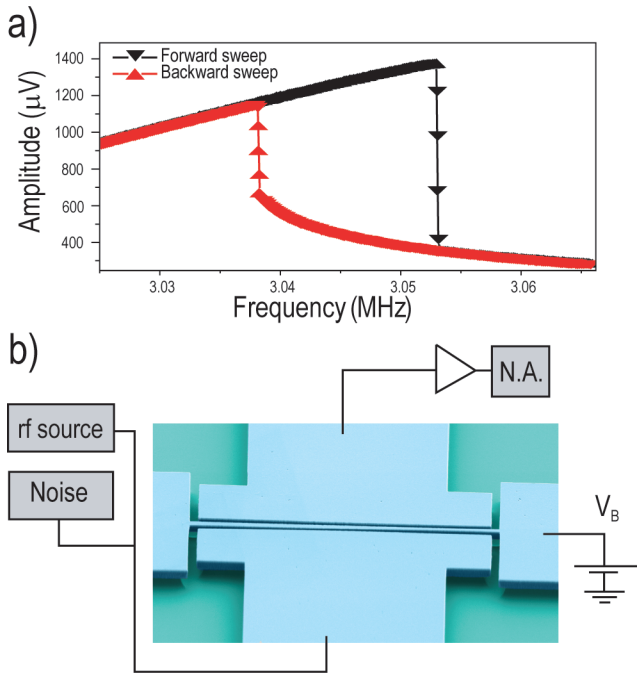

Figure 1. (a) Frequency response of the beam in the nonlinear regime showing the bistable region. (b) Experimental setup. The beam is excited with a phase modulated radio frequency (rf) source (Agilent 33220) into the bistable regime. A second signal generator adds the desired noise spectra via IQ modulation (Agilent E4338C). The current produced by the motion of the beam is amplified by a transimpedance amplifier and measured with a network analyzer (Agilent N3383A) set to continuous wave (cw) time mode to measure the time dependence of the current amplitude and phase at the excitation frequency.

This signal is monitored with a network analyzer after transimpedance amplification.

The dynamics of the system can be described by the standard Duffing equation with one degree of freedom[15]

$$\ddot{x} + \gamma\dot{x} + \omega_0^2 x + k_3 x^3 = f(t) \qquad (1)$$

where γ is a dissipation coefficient, ω_0 is the resonant angular frequency of oscillation, k_3 is the nonlinear coefficient, and $f(t)$ represents the time-dependent forcing. For small drive amplitudes the response of the beam is linear, exhibiting the standard Lorentzian line shape with a resonance frequency $f_0 = (\omega_0/2\pi) = 3$ MHz and a quality factor $Q = (\omega_0/\gamma) = 50$ (at ~0.1 Torr). As the drive amplitude is increased, the spectral response of the beam bends toward higher frequency (corresponding to $k_3 > 0$), and eventually the hysteretic regime is reached as shown in Figure 1a. This regime is reached with an applied voltage of ~70 mV corresponding to a drive power of ~1 nW.

To induce switching between these bistable amplitude states, we employ a phase modulation technique described in detail elsewhere.[11] Controlled switching can be produced by modulating the phase of the driving force with a square wave of frequency Ω: $f(t) = f_D \cos(\omega t + (\varphi_0/2)\Theta(\Omega))$, where φ_0 is the phase deviation, ω is a frequency in the bistable region, and $\Theta(\Omega)$ represents a square wave of period $2\pi/\Omega$

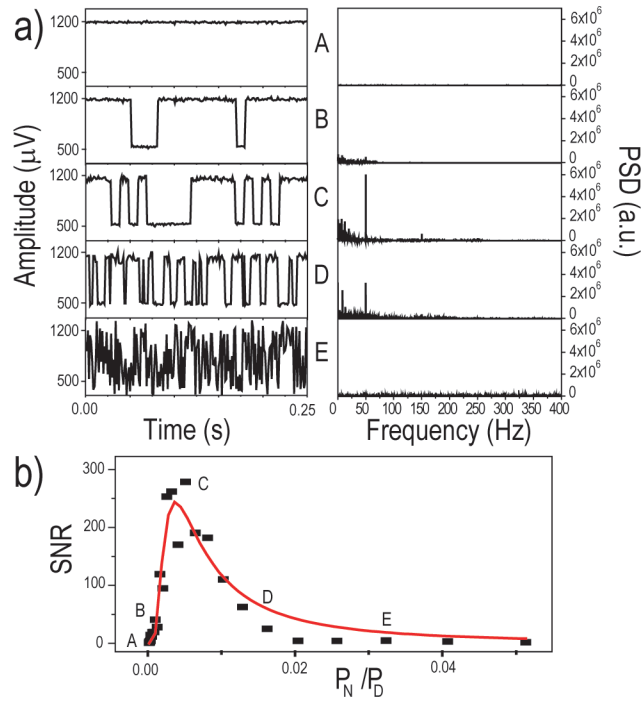

Figure 2. (a) Example of the progression of stochastic resonance. Each plot in the left panel exhibits a short, exemplary section of the time domain response for a 50 Hz modulation signal in the presence of white noise. For small noise powers, the modulation remains subthreshold, and no switching occurs (A). However, as noise power is increased (top to bottom), some sporadic switch events are induced (B), and eventually, peak switching fidelity is reached (C). Continued escalation of the noise power increases the switching rate but also leads to some incoherent switch events (D) and ultimately to completely random switching (E). Plots in the right panel display the power spectral density of each time domain measurement. At the onset of switching, peaks at odd multiples of the modulation frequency can be seen, owing to the square wave character of the beam response. (b) SNR vs noise power for the full range of measurement covered in panel a. In this plot and all following, noise power P_N is presented in units of the modulation signal power, P_D (The lettered points correspond to those featured in the above plots, and the solid line represents a fit to eq 2).

$(\Theta(\Omega) = 1$ for the first half of the period and -1 for the other). However, below a clear threshold in the value of φ_0, switching does not occur. By adding noise to a subthreshold phase deviation signal, we recover switching at the modulation frequency. Using IQ modulation to create various colored noise spectra[16] with the second signal generator, we explore the effects of noise color on stochastic resonance.

Each SR measurement begins with establishing a subthreshold phase deviation signal and verifying that in the absence of noise, the modulation fails to produce switching. Noise is then applied within a 50 kHz band encompassing the resonance of the beam, and the response for 500 periods of the modulation is recorded. Figure 2 displays typical results using white noise. Although noise-enhanced switching does not reach 100% fidelity in any of the measurements, the behavior as a function of noise power exhibits the signature of stochastic resonance (Figure 2b). Signal-to-noise ratio (SNR) is computed from the power spectrum of each time domain measurement as the ratio of the peak at the modulation frequency, $S(\Omega)$, to the background at that

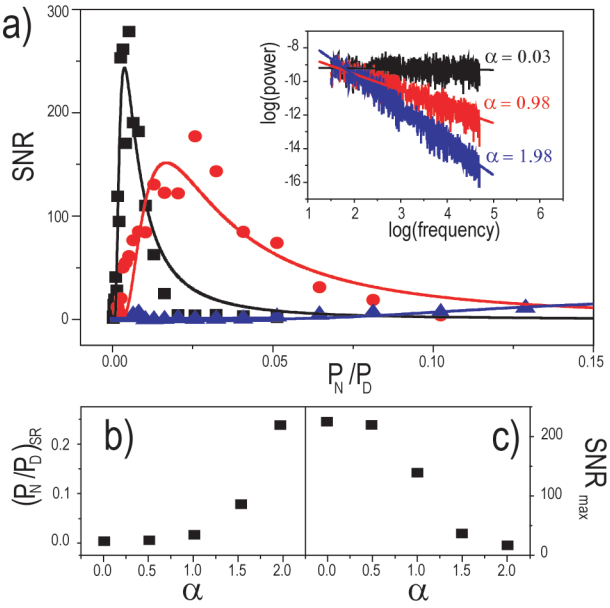

Figure 3. (a) SNR vs input noise power for three different colored noise spectra (α = 0.5 and 1.5 are removed for clarity). Solid lines depict fits to eq 2. The inset shows measured spectral shape for the three types of noise used with accompanying linear fits to the log−log plot exhibiting the experimental values of α. (c,b) Values for the peak SNR and corresponding noise power as a function of α, as extracted from the fits in panel a.

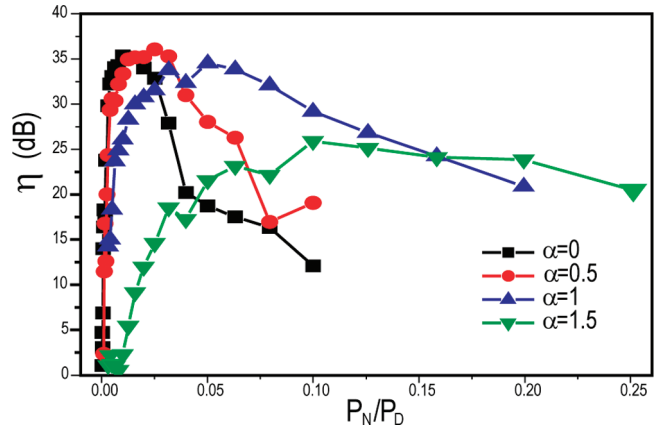

Figure 4. Spectral amplification vs input noise power for $1/f^{\alpha}$ noise with α = 0, 0.5, 1, and 1.5. The spectral amplification presents peak values of 35.3 dB at $P_N/P_D = 0.01$ for α = 0, 36.1 dB at $P_N/P_D = 0.025$ for α = 0.5, 34.6 dB at $P_N/P_D = 0.05$ for α = 1, and 25.9 dB at $P_N/P_D = 0.1$ for α = 1.5.

frequency, $N(\Omega)$. We define input noise power as the power contained within the resonance of the beam, and we express this noise power, P_N, in units of the phase-modulated drive power, P_D. Fitting with two parameters (A and B) to the well-known form for SNR[9]

$$\mathrm{SNR} = \left(\frac{A}{P_N/P_D}\right)^2 e^{-B/(P_N/P_D)} \qquad (2)$$

we find good agreement.

Applying colored noise spectra of the form $1/f^{\alpha}$ within the same bandwidth, we repeat the measurement for α ranging from 0 to 2 in steps of 0.5 (Figure 3a). Using noise spectra with increasing color, we again observe recovery of switching, though with a suppressed SNR characterized by a broadening and flattening of the resonance. Measurements on a second resonator confirm these trends. Lacking an analytical expression for SNR in the presence of $1/f^{\alpha}$ noise, we treat each spectrum as an equivalent white noise and fit to the standard form of eq 2. The peak SNR and optimum noise power extracted from these fits progress smoothly toward lower and higher values, respectively, as α increases (Figure 3b, c). These general trends are in agreement with theoretical predictions for the standard double-well potential,[17] numerical simulations of level-crossing detectors,[18] and previous experimental results.[12,19] The broadening of the SNR resonance that we observe agrees qualitatively with experimental findings using a Schmitt trigger,[19] though here we extend the approach to comprehensively study the effect of the noise exponent. Another meaningful comparison can be made with the observation of SR using $1/f^{\alpha}$ noise in a biological system, rat sensory neurons.[12] The trends that we observe adding $1/f^{\alpha}$ noise to a nanomechanical resonator, namely decrease in peak SNR and shift in the resonance with increasing noise exponent, mirror those reported in ref 12.

For a slightly different perspective on the signal amplification achieved via noise-enhanced switching, we also plot spectral amplification, η, computed as $S(\Omega)|_{P_N}/S(\Omega)|_{P_N=0}$. Figure 4 displays η for four different noise spectra as a function of applied noise level. Again, peak amplification of the switching signal occurs at increasingly large noise powers for $1/f$ noise; however, we note that the signal levels reached with α = 0.5 and 1 rival those seen with white noise, and in some cases, exceed them. Further increase in the value of α results in a sharp drop of peak signal levels as seen in Figure 4.

For further validation of these results we perform the equivalent numerical experiment by integrating the Duffing equation in the presence of the different noise colors using the modified Euler method.[20] To facilitate the numerical integration of the equation we work with the dimensionless version of eq 1, obtained by using the dimensionless displacement $z = x(k_3/m\omega_0^2)^{1/2}$ and the dimensionless time $\tau = \omega_0 t$

$$\frac{\mathrm{d}^2 z}{\mathrm{d}\tau^2} + Q^{-1}\frac{\mathrm{d}z}{\mathrm{d}\tau} + z + z^3 = \tilde{f}_D \cos\left(\tilde{\omega}\tau + \frac{\phi_o}{2}\Theta(\tilde{\Omega})\right) + \tilde{\eta}_1(\tau)\cos(\tilde{\omega}_0\tau) + \tilde{\eta}_2(t)\sin(\tilde{\omega}_0 t) \qquad (3)$$

where Q is the quality factor of the resonator, $\tilde{f}_D = f_D/\omega_0^3(k_3/m^3)^{1/2}$ the dimensionless force, and $\tilde{\omega} = \omega/\omega_0$ the dimensionless angular frequency (with the same relation for the other angular frequencies). Using the measured value for the quality factor, the force is adjusted to mimic the spectral response of the resonator. Noise of different color (produced in the same way as the noise used in the experiments) is applied encompassing the resonance of the beam in the presence of a subthreshold modulation signal. Equation 3 is then solved generating a time sequence with a duration of 500 periods of the modulation. The power spectral density

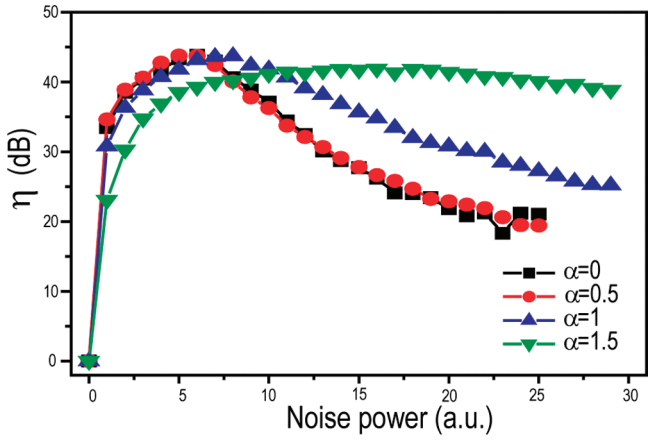

Figure 5. Spectral amplification vs input noise power for $1/f^{\alpha}$ noise with $\alpha = 0$, 0.5, 1, and 1.5 obtained by numerical simulation of the system. The simulation results show a qualitative agreement with the experiment, meaning the broadening and shift to higher powers with a less pronounced suppression of the amplification peak values.

for each noise power is calculated as the average of the FFT over 30 different noise realizations. The results obtained from the simulation agree qualitatively with the experimental results, as shown in Figure 5. As seen in the experimental data the spectral amplification peak broadens and shifts to higher powers with increasing α, although the changes here are less drastic. The simulation supports the main experimental result, meaning that the signal amplification observed with $1/f$ noise is comparable to the one obtained with white noise.

In conclusion, we observe stochastic resonance in the switching behavior of a bistable nanomechanical resonator using a wide variety of colored noise spectra. Findings suggest the monotonic suppression of achievable signal-to-noise ratio with increasing noise color, that is, α. Despite requiring larger noise powers than white noise, moderately colored $1/f^{\alpha}$ noise ($\alpha \leq 1$) proves reasonably effective at amplifying a weak modulation signal. Given the prevalence of $1/f$ noise in integrated circuitry and the continued emergence of NEMS as a viable medium for computational and memory applications, the signal enhancement seen here suggests the possible beneficial use of inherent noise to improve device performance.

Acknowledgment. We acknowledge support from NSF under the grant number EMT/NANO-0829885.

Note Added after ASAP Publication: This article was published ASAP on August 17, 2009. An Acknowledgment has been added to the paper. The correct version was published on August 21, 2009.

References

(1) Johnson, J. B. *Phy. Rev.* **1925**, *26*, 71–85.
(2) Kiss, L. L.; Szabo, G. M.; Bedding, T. R. *Mon. Not. R. Astron. Soc.* **2006**, *372*, 1721–1734.
(3) Parsons, T. *Nat. Geosci.* **2008**, *1*, 59–63.
(4) Voss, R. F. *Phys. Rev. Lett.* **1992**, *68*, 3805–3808.
(5) Kobayashi, M.; Musha, T. *IEEE Trans. Biomed. Eng.* **1982**, *29*, 456–457.
(6) Gilden, D. L.; Thornton, T.; Mallon, M. W. *Science* **1995**, *267*, 1837–1839.
(7) Kogan, Sh. *Electronic Noise and Fluctuations in Solids*; Cambridge University Press: Cambridge, 1996.
(8) Bialczak, R. C.; et al. *Phys. Rev. Lett.* **2007**, *99*, 187006.
(9) Gammaitoni, L.; Hänggi, P.; Jung, P.; Marchesoni, F. *Rev. Mod. Phys.* **1998**, *70*, 223–287.
(10) Badzey, R. L.; Zolfagharkhani, G.; Gairdazhy, A.; Mohanty, P. *Appl. Phys. Lett.* **2004**, *85*, 3587.
(11) Guerra, D. N.; Imboden, M.; Mohanty, P. *Appl. Phys. Lett.* **2008**, *93*, 033515.
(12) Nozaki, D.; Mar, D. J.; Grieg, P.; Collins, J. J. *Phys. Rev. Lett.* **1999**, *82*, 2402–2405.
(13) Badzey, R. L.; Mohanty, P. *Nature* **2005**, *437*, 995–998.
(14) Almog, R.; Zaitsev, S.; Shtempluck, O.; Buks, E. *Appl. Phys. Lett.* **2007**, *90*, 013508.
(15) Nayfeh, A. H.; Mook, D. T. *Nonlinear Oscillations*; Wiley: New York, 1979.
(16) Dunn, T.; Guerra, D. N.; Mohanty, P. *Eur. Phys. J. B* **2009**, *69*, 5.
(17) Fuentes, M. A.; Wio, H. S. *Eur. Phys. J. B* **2006**, *52*, 249–253.
(18) Makra, P.; Gingl, Z.; Fulei, T. *Phys. Lett. A* **2003**, *317*, 228–232.
(19) Kiss, L. B.; et al. *J. Stat. Phys.* **1993**, *70*, 451–462.
(20) Buchanan, J. L.; Turner, P. R. *Numerical Methods and Analysis*; McGraw-Hill: Princeton, 1992.

NL9004546